



Magnetic field effect on static antiferromagnetic order and spin excitations in the underdoped iron arsenide superconductor $\text{BaFe}_{1.92}\text{Ni}_{0.08}\text{As}_2$

Miaoyin Wang,¹ Huiqian Luo,² Meng Wang,^{1,2} Songxue Chi,^{3,4} Jose A. Rodriguez-Rivera,^{3,4}
Deepak Singh,^{3,4} Sung Chang,³ Jeffrey W. Lynn,³ and Pengcheng Dai^{1,2,5,*}

¹*Department of Physics and Astronomy, The University of Tennessee, Knoxville, Tennessee 37996-1200, USA*

²*Beijing National Laboratory for Condensed Matter Physics and Institute of Physics, Chinese Academy of Sciences, P.O. Box 603, Beijing 100190, China*

³*NIST Center for Neutron Research, National Institute of Standards and Technology, Gaithersburg, Maryland 20899, USA*

⁴*Department of Materials Science and Engineering, University of Maryland, College Park, Maryland 20899, USA*

⁵*Neutron Scattering Science Division, Oak Ridge National Laboratory, Oak Ridge, Tennessee 37831-6393, USA*

(Received 18 January 2011; revised manuscript received 9 February 2011; published 14 March 2011)

We use neutron scattering to study the magnetic-field effect on the static antiferromagnetic (AF) order and low-energy spin excitations in the underdoped iron arsenide superconductor $\text{BaFe}_{1.92}\text{Ni}_{0.08}\text{As}_2$. At zero field, superconductivity that occurs below a critical temperature of $T_c = 17$ K coincides with the appearance of a neutron spin resonance and reduction in the static ordered moment. Upon application of a ~ 10 -T magnetic field in the FeAs plane, the intensity of the resonance is reduced, accompanied by decreasing T_c and enhanced static AF scattering. These results are similar to those for some copper oxide superconductors, and demonstrate that the static AF order is a competing phase to superconductivity in $\text{BaFe}_{1.92}\text{Ni}_{0.08}\text{As}_2$.

DOI: [10.1103/PhysRevB.83.094516](https://doi.org/10.1103/PhysRevB.83.094516)

PACS number(s): 74.25.Ha, 74.70.-b, 78.70.Nx

I. INTRODUCTION

The parent compounds of iron arsenide superconductors exhibit static antiferromagnetic (AF) order with a simple collinear spin structure as shown in Fig. 1(a).¹⁻³ Since superconductivity in iron arsenides can arise from electron or hole doping of their AF parent compounds,^{4,5} it is generally believed that magnetism plays an important role in the superconductivity of these materials.⁶⁻¹⁰ In one class of electron-doped iron-arsenide-based superconductors, $\text{BaFe}_{2-x}(\text{Co,Ni})_x\text{As}_2$,^{11,12} superconductivity and static AF order can coexist in the underdoped regime.¹³⁻¹⁵ Subsequent neutron scattering experiments on these samples reveal that the occurrence of superconductivity is accompanied by a reduction in the static AF Bragg intensity and the appearance of a neutron spin resonance in the magnetic excitation spectra.¹⁶⁻¹⁸ Theoretically, it has been argued that the coexisting static AF order and superconductivity are inconsistent with conventional BCS theory but compatible with electron pairing mediated by quasiparticle excitations between sign-reversed s -wave hole-like pockets around the Γ point and the electron-like Fermi pockets around the M point (the so-called s^\pm pairing symmetry).¹⁹⁻²⁴ In this pure itinerant picture, electrons that form the ordered moment also contribute to the superconducting condensation, and the AF order and superconductivity thus coexist microscopically.^{23,24} If the static AF order in $\text{BaFe}_{2-x}(\text{Co,Ni})_x\text{As}_2$ also has local moment contributions,^{25,26} the magnetically ordered phase can coexist much more easily with superconductivity but the ordered moment should not be affected by superconductivity.²⁴

One way to test the interplay between magnetism and superconductivity is to use the magnetic field as a tuning parameter. If the static AF order in the underdoped $\text{BaFe}_{2-x}(\text{Co,Ni})_x\text{As}_2$ indeed coexists and competes with superconductivity,¹⁵⁻¹⁸ application of a magnetic field that suppresses superconductivity should also enhance the static AF order, much like that of the electron-doped copper oxide superconductors.^{27,28} On the

other hand, if the static AF order in $\text{BaFe}_{2-x}(\text{Co,Ni})_x\text{As}_2$ is chemically phase separated from the superconducting parts of the sample, then the application of a magnetic field should reduce the AF-ordered moment, as has been found in chemically phase-separated $\text{Ba}_{1-x}\text{K}_x\text{Fe}_2\text{As}_2$.²⁹ Neutrons cannot directly probe the microscopic nature of the coexisting state between static AF order and superconductivity,¹⁶⁻¹⁸ but neutron scattering experiments in a magnetic field will allow a direct comparison of the effect of a field on the superconductivity and static AF order. In previous neutron-scattering experiments on optimally doped iron arsenide $\text{BaFe}_{0.9}\text{Ni}_{0.1}\text{As}_2$,³⁰ a c -axis-aligned magnetic field of up to 14.5 T has been found to suppress the intensity of the neutron spin resonance and shift it to a lower energy corresponding to the field-induced reduction in the critical temperature T_c . Although such a field also reduces the magnitude of the spin gap, it is not sufficient to induce static AF order.³⁰ As a consequence, it is not clear if the static AF order is a competing phase to superconductivity. In a separate neutron scattering on an iron chalcogenide $\text{FeTe}_{0.5}\text{Se}_{0.5}$ superconductor,³¹ a 7-T magnetic field parallel to the a - b plane was found to reduce the intensity of the resonance. Similar to the results on $\text{BaFe}_{0.9}\text{Ni}_{0.1}\text{As}_2$,³⁰ a 7-T field was also insufficient to induce the static AF order in the sample.³¹

In this paper, we report neutron scattering studies on the static AF order and spin excitations of underdoped $\text{BaFe}_{1.92}\text{Ni}_{0.08}\text{As}_2$ [$T_c = 17$ K, Fig. 1(d)] under the influence of an applied magnetic field. At zero field, previous neutron scattering experiments on similar samples have shown that the static AF-ordered moment is reduced at the onset of superconductivity, together with the appearance of a neutron spin resonance in the magnetic excitation spectra.¹⁶⁻¹⁸ We find that the static AF order in $\text{BaFe}_{1.92}\text{Ni}_{0.08}\text{As}_2$ is not limited by instrument resolution and has a spin-spin correlation length shorter than the lattice correlation length. Upon application of a magnetic field in the FeAs plane, the static AF order is enhanced below T_c , but it is not affected in the temperature

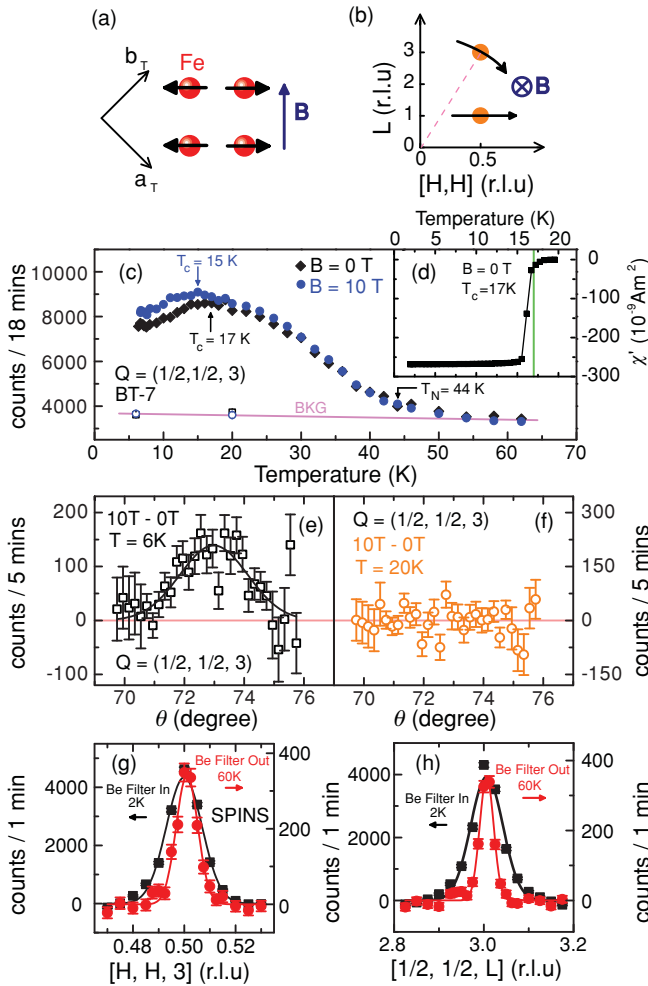


FIG. 1. (Color online) (a) The antiferromagnetic spin structure of the undoped parent compound BaFe_2As_2 and the direction of applied field. (b) The reciprocal space probed in the present experiment and the direction of applied field. (c) Temperature dependence of the AF Bragg peak at $(0.5, 0.5, 3)$ at zero field and at the 10-T in-plane field. The data were taken on BT-7 and showed $T_N = 44$ K. The background scattering has no temperature or field dependence. (d) Temperature dependence of the Meissner and shielding signals on thin slabs of $\text{BaFe}_{1.92}\text{Ni}_{0.08}\text{As}_2$. These measurements were taken in zero-field cooling (ZFC) with a 5-Oe applied field along the thin slab's direction. (e) The field-on subtract field-off rocking-curve scan through the $(0.5, 0.5, 3)$ AF Bragg peak at 6 K. The positive scattering centered at the correct θ angle indicates that the field-induced effect occurs at the $(0.5, 0.5, 3)$ AF Bragg position. (f) Identical rocking-curve scans at 20 K, clearly indicating that the applied field has no observable effect on the static AF order below T_N and above T_c . (g) Black squares indicate a high-resolution scan along the $[H, H, 3]$ direction in the AF-ordered state. The red circles show the identical scan above T_N without the cold Be filter, which gives $\lambda/2$ scattering from the lattice structural Bragg peak $(1, 1, 6)$. (h) Similar scans along the $[0.5, 0.5, L]$ direction.

range below the Néel temperature T_N and above T_c ($T_c < T < T_N$). The enhancement of the static AF order is accompanied by a suppression of both the superconducting T_c and the intensity of the neutron spin resonance. These results are consistent with a competing static AF order and superconductivity,

and they suggest that the interplay between magnetism and superconductivity in iron arsenide superconductors is similar in many ways to that for copper oxide superconductors.

II. EXPERIMENTAL DETAILS

In recent inelastic neutron scattering experiments on underdoped $\text{BaFe}_{1.906}\text{Co}_{0.094}\text{As}_2$ ($T_c = 15$ K),¹⁶ $\text{BaFe}_{1.92}\text{Co}_{0.08}\text{As}_2$ ($T_c = 11$ K),¹⁷ and $\text{BaFe}_{2-x}\text{Ni}_x\text{As}_2$ ¹⁸ superconductors, the static AF order was found to coexist with superconductivity, while cooling below the T_c 's in these samples induced a weak neutron spin resonance in the magnetic excitation spectra at the expense of the AF Bragg peak intensity. For $\text{BaFe}_{1.92}\text{Ni}_{0.08}\text{As}_2$ with $T_c = 17$ K [Fig. 1(d)], the static AF order occurs below $T_N = 44$ K as shown in Fig. 1(c). To study the effect of an in-plane magnetic field on the static AF order and spin excitations, we have carried out neutron scattering experiments on the BT-7 thermal and the spin-polarized inelastic neutron (SPINS) cold triple-axis spectrometers¹⁸ and on the Multi Axis Crystal Spectrometer (MACS)³² at the National Institute for Science and Technology (NIST) Center for Neutron Research. We defined the wave vector Q at (q_x, q_y, q_z) as $(H, K, L) = (q_x a/2\pi, q_y b/2\pi, q_z c/2\pi)$ reciprocal lattice units (rlu) using the tetragonal nuclear unit cell, where $a = 3.89$ Å, $b = 3.89$ Å, and $c = 12.77$ Å. We coaligned about 5 g of single-crystal $\text{BaFe}_{1.92}\text{Co}_{0.08}\text{As}_2$ in the $[H, H, L]$ horizontal scattering plane (with mosaicity $\sim 3^\circ$) and put our samples inside either a liquid He cryostat or a 12-T vertical-field magnet. For thermal triple-axis measurements on the BT-7, we used pyrolytic graphite (PG) as the monochromator and analyzer with typical collimations of open-40'-S-40'-120' and the 15-T superconducting magnet system. The final neutron energy was chosen to be $E_f = 13.5$ meV with a PG filter before the analyzer. For cold-neutron SPINS and MACS measurements, we chose a final neutron energy of $E_f = 5.0$ meV with cold Be filters to eliminate $\lambda/2$ scattering. Figure 1(a) shows the spin structure of the parent compound, and Fig. 1(b) illustrates the reciprocal space probed in the experiments.

III. RESULTS AND DISCUSSION

We first discuss our neutron scattering results on $\text{BaFe}_{1.92}\text{Ni}_{0.08}\text{As}_2$ at zero field. The solid diamonds in Fig. 1(c) show the temperature dependence of the magnetic scattering at $Q = (0.5, 0.5, 3)$. Consistent with earlier results on underdoped FeAs-based superconductors,^{16–18} $\text{BaFe}_{1.92}\text{Ni}_{0.08}\text{As}_2$ orders antiferromagnetically below a Néel temperature of $T_N = 44$ K, and the magnetic Bragg intensity decreases below the onset of the superconducting T_c . To test if the AF order in $\text{BaFe}_{1.92}\text{Ni}_{0.08}\text{As}_2$ is indeed long range and limited by instrument resolution, we carried out high-resolution measurements on SPINS. First, we performed Q -scans along the $[H, H, 3]$ and $[0.5, 0.5, L]$ directions in the AF-ordered state at 2 K with a cold Be filter before the analyzer to eliminate $\lambda/2$ scattering [black squares in Figs. 1(g) and 1(h)]. We then carried out identical measurements in the paramagnetic state ($T = 60$ K) without the Be filter before the analyzer using $\lambda/2$ from the $(1, 1, 6)$ nuclear Bragg peak as a probe of the instrumental resolution [red circles in Figs. 1(g) and 1(h)]. The outcome clearly suggests that the AF order in $\text{BaFe}_{1.92}\text{Ni}_{0.08}\text{As}_2$ is not limited

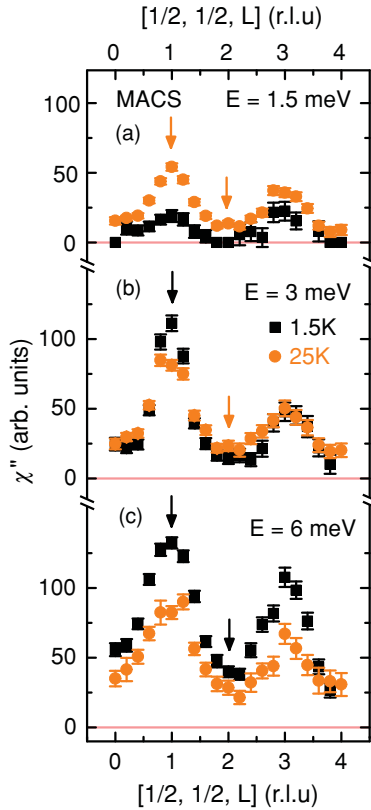


FIG. 2. (Color online) Temperature dependence of the imaginary part of the dynamic susceptibility, $\chi''(Q, \omega)$, after subtracting the background scattering and correcting for the Bose population factor. (a) Q -scans at $E = 1.5$ meV along the $[0.5, 0.5, L]$ direction above and below T_c . The data show clear L -direction sinusoidal modulation. (b) Similar scans at an energy just below the resonance ($E = 3$ meV). (c) Q -scans at the resonance energy of $E = 6$ meV. The intensity gain below T_c is clearly not uniform at different L values.

by instrument resolution. Solid lines in Fig. 1(g) and 1(h) are Gaussian fits to the peaks on linear backgrounds, where $I = \text{bkgd} + I_0 \exp[-(H - H_0)^2 / (2\sigma^2)]$ and the full-width-half-maximum (FWHM) = 2.3548σ . The in-plane measured peak and instrument resolution FWHMs are 0.0165 and 0.0099 rlu, respectively. Along the c axis, the in-plane measured peaks and the instrument resolution are 0.0843 and 0.0363 rlu, respectively. To estimate the spin-spin coherence length (ξ), we use the Fourier transform of the Gaussian peaks. For the $[H, H, L]$ scattering zone, the in-plane and c -axis spin-spin coherence lengths are $\xi = [\sqrt{\ln(2)/\pi}](a/\sigma)$ and $\xi = [\sqrt{2\ln(2)/\pi}](c/\sigma)$, respectively.²⁷ By deconvoluting the instrument effect, we estimate that the static AF spin-spin correlation lengths at $T = 2$ K are $\xi = 183 \pm 15$ Å in the FeAs plane, and $\xi = 148 \pm 10$ Å along the c axis. For comparison, we note that the static AF order in $\text{Ba}(\text{Fe}_{0.953}\text{Co}_{0.047})_2\text{As}_2$ with $T_N = 47$ K and $T_c = 17$ K¹⁶ is long range and limited by instrument resolution.³³

To see if the static AF order in $\text{BaFe}_{1.92}\text{Ni}_{0.08}\text{As}_2$ can be enhanced by application of a magnetic field, we carried out detailed temperature-dependent measurements at the AF Bragg peak position $Q = (0.5, 0.5, 3)$ with and without a 10-T magnetic field applied along the $[1, -1, 0]$ direction

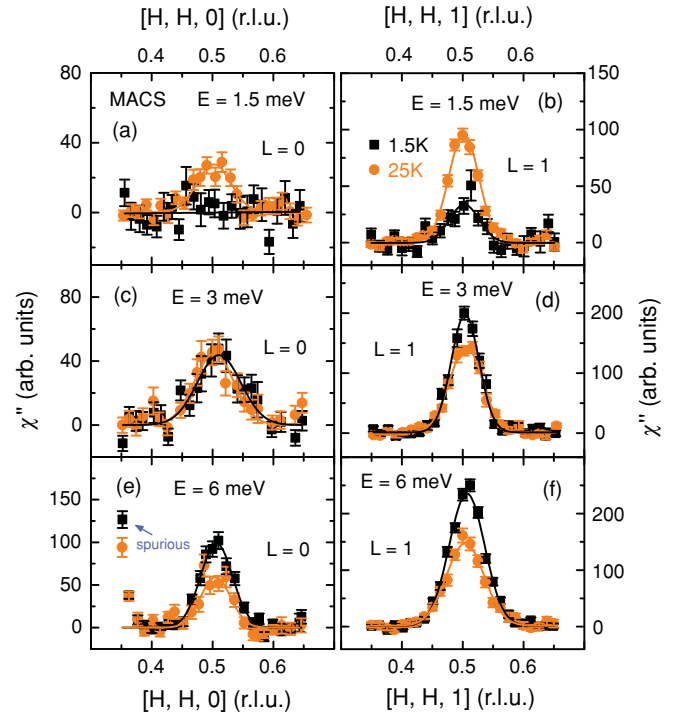


FIG. 3. (Color online) Temperature dependence of $\chi''(Q, \omega)$ along the $[H, H, 0]$ and $[H, H, 1]$ directions. (a) Constant-energy scans at $E = 1.5$ meV along the $[H, H, 0]$ direction across T_c . A clean spin gap is seen at this energy. (b) Identical scans along the $[H, H, 1]$ direction, which show clear magnetic scattering centered at $Q = (0.5, 0.5, 1)$ in the superconducting state. (c) Constant-energy scans at $E = 3$ meV show no change in χ'' below and above T_c at $Q = (0.5, 0.5, 0)$. (d) The scattering clearly increases at $Q = (0.5, 0.5, 1)$ below T_c . (e) Constant-energy scans at $E = 6$ meV. The peak at $Q = (0.3, 0.3, 0)$ is spurious. (f) Similar scans at $E = 6$ meV across $Q = (0.5, 0.5, 1)$. Superconductivity clearly induces more magnetic scattering at $Q = (0.5, 0.5, 1)$ than at $Q = (0.5, 0.5, 0)$.

[Fig. 1(c)]. While a 10-T in-plane magnetic field has no observable effect on the Néel temperature and magnetic scattering above 20 K, it clearly enhances the magnetic scattering for temperatures below T_c compared to that of the zero-field data. Figures 1(e) and 1(f) show the rocking curves of the field-on-field-off difference plots at 5 and 20 K, respectively. While a 10-T magnetic field has no influence on the static AF order at 20 K [Fig. 1(f)], it induces additional magnetic scattering at $(0.5, 0.5, 3)$ below T_c [Fig. 1(e)].

In previous neutron scattering work on $\text{BaFe}_{2-x}\text{Ni}_x\text{As}_2$,^{18,34-36} energy-dispersive neutron spin resonances were found in the underdoped samples. However, it is not clear how spin excitations evolve and respond to superconductivity at energies below the resonance.¹⁸ Figure 2 summarizes the effect of superconductivity on the c -axis modulations of the spin dynamic susceptibility $\chi''(Q, \omega)$ at different energies obtained on MACS. At $E = 1.5$ meV, $\chi''(Q, \omega)$ displays a clear sinusoidal modulation along the L direction centered at $L = 1, 3, \dots$ in the normal state at $T = 25$ K. Upon entering into the superconducting state ($T = 1.5$ K), the scattering at $L = 0, 2, 4, \dots$ vanishes, indicating the presence of a spin gap while there is still magnetic scattering at $L = 1, 3, \dots$. These results are

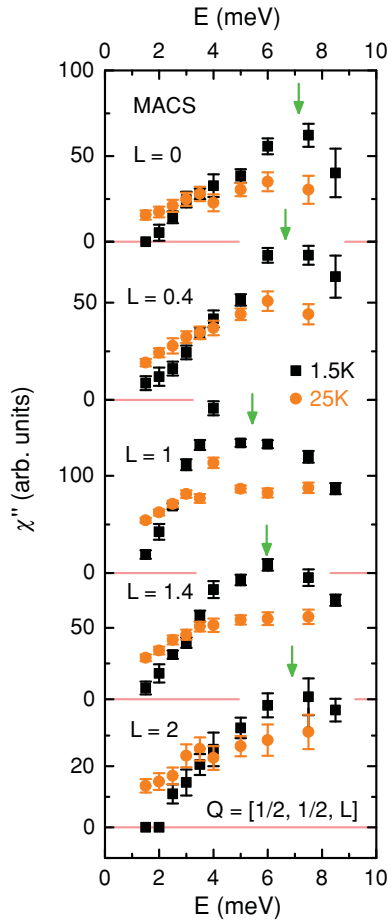


FIG. 4. (Color online) Energy dependence of the dynamic susceptibility $\chi''(\omega)$ above and below T_c for wave vectors $Q = (0.5, 0.5, L)$ with $L = 0, 0.4, 1, 1.4, 2$. In the normal state, $\chi''(\omega)$ increases with increasing energy at all L values. On entering into the superconducting state, the neutron spin resonance develops and exhibits dispersion, occurring at different energies for different L values as marked by the vertical arrows.

confirmed by constant-energy scans along the $[H, H, L]$ direction with $L = 0, 1$ [Figs. 3(a) and 3(b)], and they are similar to the L dependence of the spin gaps for the optimally electron-^{35,36} and hole-doped³⁷ FeAs-based superconductors.

At an energy just below the resonance ($E = 3$ meV), $\chi''(Q)$ still has a strong L modulation in both the normal and superconducting states [Fig. 2(b)]. On cooling from 25 to 1.5 K, $\chi''(Q)$ at $Q = (0.5, 0.5, 1)$ is enhanced slightly but undergoes no change at $Q = (0.5, 0.5, 0)$. Constant-energy scans in Figs. 3(c) and 3(d) confirm these results. For an energy transfer near the resonance ($E = 6$ meV), superconductivity enhances $\chi''(Q)$ at all L values, as shown in Fig. 2(c). Constant-energy scans in Figs. 3(e) and 3(f) also show that the magnetic intensity gain at $L = 0$ is smaller than that at $L = 1$. This is consistent with the dispersive nature of the resonance, where the mode shifts from ~ 7.5 meV at $L = 0, 2$ to ~ 5.8 meV at $L = 1$ shown in Fig. 4, similar to previous work on Co-doped $\text{BaF}_{1.906}\text{Co}_{0.094}\text{As}_2$.³⁸

To determine if the enhanced static AF order in Fig. 1(c) under a magnetic field is compensated by a reduction in the intensity of the resonance and low-energy spin excitations, we

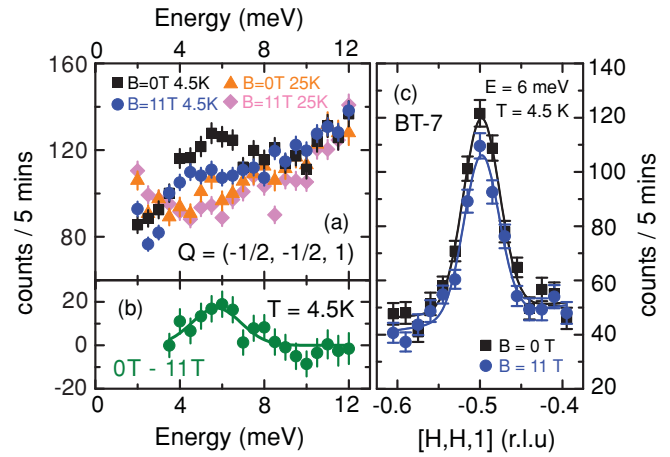


FIG. 5. (Color online) Energy and wave-vector dependence of the spin excitations as a function of an applied magnetic field in the FeAs plane. (a) Constant- Q scans at $Q = (-0.5, -0.5, 1)$ below and above T_c at zero field and at the 11-T in-plane field. Inspection of the raw data clearly reveals the reduction of the resonance intensity under the field at $T = 4.5$ K. (b) The field-off-field-on difference plot at $T = 4.5$ K shows that the magnetic scattering near the resonance energy is affected most by the applied field. (c) Constant-energy scans at the resonance energy for the zero and the 11-T fields. The field-induced reduction in magnetic scattering occurs at the AF wave vector $Q = (-0.5, -0.5, 1)$.

carried out inelastic neutron scattering measurements under the influence of a magnetic field. Figure 5(a) shows constant- Q scans carried out below and above T_c in zero field and in the 11-T in-plane field at $Q = (-0.5, -0.5, 1)$. At zero field, the scan at 4.5 K shows a clear resonance peak near 6 meV. Upon application of an 11-T in-plane field, the intensity of the mode is reduced [Fig. 5(a)]. The zero and 11-T field-difference plot at 4.5 K in Fig. 5(b) shows a peak centered at 6 meV. Therefore, while a 14-T field applied along the c axis can suppress the intensity and reduce the energy of the resonance, a 11-T field applied in the FeAs plane only reduces the intensity of the resonance and does not affect the energy of the mode. This can be explained naturally by the vortex lattice effects in superconductors. A c -axis-aligned magnetic field can suppress superconductivity much more efficiently than an in-plane field because the former induces supercurrent in the FeAs planes, while vortex lattices in an in-plane field are present between the superconducting FeAs planes. Figure 5(c) shows constant-energy scans in the superconducting state with and without the applied magnetic field. The effect of an applied field is to suppress magnetic scattering centered at the AF wave vector near the resonance energy.

Figure 6 shows the temperature dependence of the resonance at fields of zero and 11 T. At zero field, the intensity of the mode increases gradually below $T_c = 17$ K [Fig. 6(a)]. Under the influence of a 11-T field in the FeAs plane, the resonance intensity starts to increase below about 15 K [Fig. 6(b)]. The reduced T_c in the in-plane field for the resonance is consistent with the reduction in the AF Bragg intensity, as shown in Fig. 6(c). These results are also consistent with the expected T_c reduction from the transport measurements for similar T_c Co-doped materials.³⁹ If we assume that the

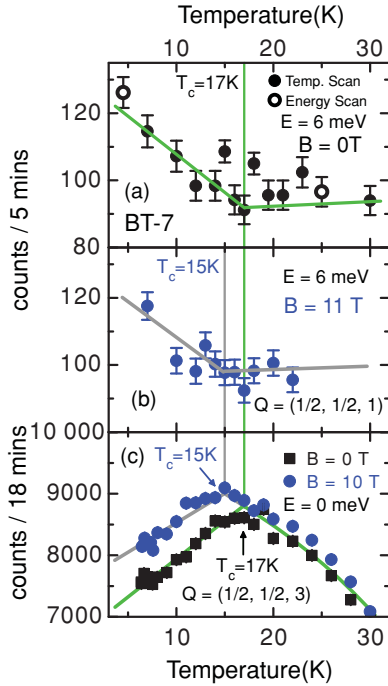


FIG. 6. (Color online) Temperature dependence of the resonance and elastic scattering at zero field and at the 11-T in-plane field. (a) Temperature dependence of the $E = 6$ meV scattering in zero field at $Q = (0.5, 0.5, 1)$ for $\text{BaFe}_{1.92}\text{Ni}_{0.08}\text{As}_2$. The scattering increases in intensity below the T_c of 17 K. (b) Identical temperature dependence of the $E = 6$ meV scattering under the 11-T field. The field-induced T_c has now shifted to 15 K. (c) Expanded plot of the elastic magnetic scattering in zero field and in the 11-T field. The data confirm the shift in T_c with a nonzero field.

resonance is a direct probe for measuring electron pairing and superconductivity in iron arsenide superconductors, then the observation of the elastic magnetic intensity gain at the expense of the resonance provides direct evidence that the static AF order in underdoped $\text{BaFe}_{1.92}\text{Ni}_{0.08}\text{As}_2$ is competing with superconductivity.

We now discuss the implications of our results and compare them with that of the magnetic-field effect in copper oxide superconductors. For the single-layer hole-doped cuprate $\text{La}_{2-x}\text{Sr}_x\text{CuO}_4$ near a doping of $x = 0.125$ application of a magnetic field can enhance the static long-range AF order.^{40–42} These results were initially interpreted as due to antiferromagnetism within the vortex cores of the superconductors under the field,⁴² but they have since been understood as being due to proximity to the quantum critical point separating a purely superconducting phase from a superconducting-antiferromagnetism coexisting phase.^{43,44} For the bilayer hole-doped cuprate $\text{YBa}_2\text{Cu}_3\text{O}_{6+x}$, while the initial neutron scattering experiments have shown that a field can suppress the intensity of the resonance,⁴⁵ the enhanced static order under a field has only recently been observed in underdoped $\text{YBa}_2\text{Cu}_3\text{O}_{6.45}$ ⁴⁶ and is not a universal phenomenon.⁴⁷ In the case of electron-doped cuprates, the enhanced static AF order under a field²⁷ is compensated by suppressing the intensity of the resonance.²⁸

The observation of a field-induced enhancement of the static AF order at the expense of the resonance in the underdoped iron arsenide superconductor $\text{BaFe}_{1.92}\text{Ni}_{0.08}\text{As}_2$ is similar to the field-induced effects on the static AF order and resonance in some of the cuprate superconductors,^{40–42,44,46} particularly the electron-doped materials.^{27,28} Although our results indicate a competing static AF order with superconductivity, it is still unclear whether the static AF order in $\text{BaFe}_{1.92}\text{Ni}_{0.08}\text{As}_2$ microscopically coexists with superconductivity as theoretically envisioned.^{23,24} In recent muon spin rotation (μSR) experiments on underdoped $\text{BaFe}_{2-x}\text{Co}_x\text{As}_2$ with coexisting static AF and superconducting phases, the local magnetic field detected by muons does not show a noticeable reduction below T_c .⁴⁸ Since muons are local probes, this result suggests that the static AF moment of the system does not decrease below T_c . Therefore, the coexisting AF and superconducting phases might be mesoscopic, where superconductivity and AF order are intertwined on a very short length scale and live in separate regions. The relevant length parameter for superconducting regions is the superconducting coherence length, which is on the order of 20 Å.³⁹ On the other hand, the propagation of the field from the static Fe moment to the muon site is due to the dipolar interaction, which is much shorter than the penetration depth and dies away in about 20 Å.⁴⁹ If the width of the superconducting river is smaller than the propagation range of the dipolar field, then the muons in the river regions can still feel the static internal field from the AF-ordered background. In this scenario, application of a magnetic field that suppresses the superconducting parts of the sample enhances the static AF phase through a volume fraction change (and thus the reduction in the AF Bragg peak intensity) without changing the static ordered moment (i.e., no change in the local field seen by μSR). While this picture is consistent with the observation that the static AF order in $\text{BaFe}_{1.92}\text{Ni}_{0.08}\text{As}_2$ is not resolution limited [Figs. 1(g) and 1(h)], it is inconsistent with the unchanged static spin-spin correlation lengths across T_c in $\text{BaFe}_{1.92}\text{Co}_{0.08}\text{As}_2$.¹⁷ Furthermore, recent high-resolution soft X-ray resonant magnetic scattering results suggest that the static AF order in $\text{BaFe}_{1.906}\text{Co}_{0.094}\text{As}_2$ is truly long-ranged.³³ Clearly, more systematic high-resolution neutron diffraction measurements are necessary to clarify the nature of the static AF-ordered phase and its coexistence with superconductivity in $\text{BaFe}_{2-x}(\text{Co},\text{Ni})_x\text{As}_2$.

IV. CONCLUSIONS

In summary, we have determined the effects of an in-plane magnetic field on the static AF order and spin excitations of the underdoped $\text{BaFe}_{1.92}\text{Ni}_{0.08}\text{As}_2$ superconductor. At zero field, the system orders antiferromagnetically below about 44 K but the order is not truly long-ranged and limited by instrument resolution. The spin excitations display a sinusoidal modulation along the c axis and form a dispersive neutron spin resonance associated with superconductivity as reported in earlier works.^{18,34,36} While application of a magnetic field in the FeAs plane has no observable effect on the static AF order below T_N and above T_c , it clearly enhances the zero-field static AF order at the expense of the neutron spin resonance. Our results provide direct evidence that the static AF order is a competing phase to superconductivity. However, the present

neutron scattering data cannot conclusively determine if the static AF order in $\text{BaFe}_{1.92}\text{Ni}_{0.08}\text{As}_2$ is microscopically or mesoscopically coexisting with superconductivity.

ACKNOWLEDGMENTS

We are grateful to Y. J. Uemura, G. M. Luke, and M. D. Lumsden for helpful discussions. The neutron

scattering part of this work at the University of Tennessee/Oak Ridge National Laboratories is supported by the US National Science Foundation Grant No. DMR-0756568 and by the US Department of Energy, Division of Scientific User Facilities. The single-crystal growth and neutron scattering work at the Institute of Physics is supported by the Natural Science Foundation of China, the Ministry of Science and Technology of China (973 Project No. 2011CBA00110), and the Chinese Academy of Sciences.

*pdai@utk.edu

- ¹C. de la Cruz *et al.*, *Nature (London)* **453**, 899 (2008).
- ²J. Zhao *et al.*, *Nature Mater.* **7**, 953 (2008).
- ³Q. Huang, Y. Qiu, W. Bao, M. A. Green, J. W. Lynn, Y. C. Gasparovic, T. Wu, G. Wu, and X. H. Chen, *Phys. Rev. Lett.* **101**, 257003 (2008).
- ⁴Y. Kamihara, T. Watanabe, M. Hirano, and H. Hosono, *J. Am. Chem. Soc.* **130**, 3296 (2008).
- ⁵M. Rotter, M. Tegel, and D. Johrendt, *Phys. Rev. Lett.* **101**, 107006 (2008).
- ⁶I. I. Mazin, D. J. Singh, M. D. Johannes, and M. H. Du, *Phys. Rev. Lett.* **101**, 057003 (2008).
- ⁷A. V. Chubukov, *Physica C* **469**, 640 (2009).
- ⁸F. Wang, H. Zhai, Y. Ran, A. Vishwanath, and D.-H. Lee, *Phys. Rev. Lett.* **102**, 047005 (2009).
- ⁹V. Cvetkovic and Z. Tesanovic, *Eur. Phys. Lett.* **85**, 37002 (2009).
- ¹⁰A. Moreo, M. Daghofer, J. A. Riera, and E. Dagotto, *Phys. Rev. B* **79**, 134502 (2009).
- ¹¹A. S. Sefat, R. Jin, M. A. McGuire, B. C. Sales, D. J. Singh, and D. Mandrus, *Phys. Rev. Lett.* **101**, 117004 (2008).
- ¹²L. J. Li *et al.*, *New J. Phys.* **11**, 025008 (2009).
- ¹³N. Ni, M. E. Tillman, J.-Q. Yan, A. Kracher, S. T. Hannahs, S. L. Budko, and P. C. Canfield, *Phys. Rev. B* **78**, 214515 (2008).
- ¹⁴J.-H. Chu, J. G. Analytis, C. Kucharczyk, and I. R. Fisher, *Phys. Rev. B* **79**, 014506 (2009).
- ¹⁵C. Lester, J.-H. Chu, J. G. Analytis, S. C. Capelli, A. S. Erickson, C. L. Condon, M. F. Toney, I. R. Fisher, and S. M. Hayden, *Phys. Rev. B* **79**, 144523 (2009).
- ¹⁶D. K. Pratt, W. Tian, A. Kreyssig, J. L. Zarestky, S. Nandi, N. Ni, S. L. Budko, P. C. Canfield, A. I. Goldman, and R. J. McQueeney, *Phys. Rev. Lett.* **103**, 087001 (2009).
- ¹⁷A. D. Christianson, M. D. Lumsden, S. E. Nagler, G. J. MacDougall, M. A. McGuire, A. S. Sefat, R. Jin, B. C. Sales, and D. Mandrus, *Phys. Rev. Lett.* **103**, 087002 (2009).
- ¹⁸M. Wang, H. Luo, J. Zhao, C. Zhang, M. Wang, K. Marty, S. Chi, J. W. Lynn, A. Schneidewind, S. Li, and P. Dai, *Phys. Rev. B* **81**, 174524 (2010).
- ¹⁹I. I. Mazin and J. Schmalian, *Physica C* **469**, 614 (2009).
- ²⁰T. A. Maier and D. J. Scalapino, *Phys. Rev. B* **78**, 020514(R) (2008).
- ²¹T. A. Maier, S. Graser, D. J. Scalapino, and P. Hirschfeld, *Phys. Rev. B* **79**, 134520 (2009).
- ²²M. M. Korshunov and I. Eremin, *Phys. Rev. B* **78**, 140509(R) (2008).
- ²³R. M. Fernandes *et al.*, *Phys. Rev. B* **81**, 140501(R) (2010).
- ²⁴R. M. Fernandes and J. Schmalian, *Phys. Rev. B* **82**, 014521 (2010).
- ²⁵C. Fang, H. Yao, W.-F. Tsai, J. P. Hu, and S. A. Kivelson, *Phys. Rev. B* **77**, 224509 (2008).
- ²⁶C. Xu, M. Müller, and S. Sachdev, *Phys. Rev. B* **78**, 020501 (2008).
- ²⁷H. J. Kang, P. Dai, H. A. Mook, D. N. Argyriou, V. Sikolenko, J. W. Lynn, Y. Kurita, S. Komiya, and Y. Ando, *Phys. Rev. B* **71**, 214512 (2005).
- ²⁸S. D. Wilson, S. Li, J. Zhao, G. Mu, H.-H. Wen, J. W. Lynn, P. G. Freeman, L.-P. Regnault, K. Habicht, and P. Dai, *Proc. Natl. Acad. Sci. USA* **104**, 15259 (2007).
- ²⁹J. T. Park *et al.*, *Phys. Rev. Lett.* **102**, 117006 (2009).
- ³⁰J. Zhao, L.-P. Regnault, C. L. Zhang, M. Y. Wang, Z. C. Li, F. Zhou, Z. X. Zhao, C. Fang, J. P. Hu, and P. C. Dai, *Phys. Rev. B* **81**, 180505(R) (2010).
- ³¹J. S. Wen, G. Y. Xu, Z. J. Xu, Z. W. Lin, Q. Li, Y. Chen, S. X. Chi, G. D. Gu, and J. M. Tranquada, *Phys. Rev. B* **81**, 100513 (2010).
- ³²J. A. Rodriguez *et al.*, *Meas. Sci. Technol.* **19**, 034023 (2008).
- ³³M. G. Kim *et al.*, *Phys. Rev. B* **82**, 180412(R) (2010).
- ³⁴S. X. Chi *et al.*, *Phys. Rev. Lett.* **102**, 107006 (2009).
- ³⁵S. L. Li, Y. Chen, S. Chang, J. W. Lynn, L. J. Li, Y. K. Luo, G. H. Cao, Z. A. Xu, and P. C. Dai, *Phys. Rev. B* **79**, 174527 (2009).
- ³⁶J. T. Park *et al.*, *Phys. Rev. B* **82**, 134503 (2010).
- ³⁷C. L. Zhang *et al.*, e-print arXiv:1012.4065.
- ³⁸D. K. Pratt *et al.*, *Phys. Rev. B* **81**, 140510 (2010).
- ³⁹A. Yamamoto *et al.*, *App. Phys. Lett.* **94**, 062511 (2009).
- ⁴⁰S. Katano, M. Sato, K. Yamada, T. Suzuki, and T. Fukase, *Phys. Rev. B* **62**, 14677(R) (2000).
- ⁴¹B. Khaykovich, Y. S. Lee, R. W. Erwin, S.-H. Lee, S. Wakimoto, K. J. Thomas, M. A. Kastner, and R. J. Birgeneau, *Phys. Rev. B* **66**, 014528 (2002).
- ⁴²B. Lake *et al.*, *Nature (London)* **415**, 299 (2002).
- ⁴³Y. Zhang, E. Demler, and S. Sachdev, *Phys. Rev. B* **66**, 094501 (2002).
- ⁴⁴J. Chang *et al.*, *Phys. Rev. B* **78**, 104525 (2008).
- ⁴⁵P. C. Dai, H. A. Mook, G. Aeppli, S. M. Hayden, and F. Doğan, *Nature (London)* **406**, 965 (2000).
- ⁴⁶D. Haug *et al.*, *Phys. Rev. Lett.* **103**, 017001 (2009).
- ⁴⁷C. Stock, W. J. L. Buyers, K. C. Rule, J.-H. Chung, R. Liang, D. Bonn, and W. N. Hardy, *Phys. Rev. B* **79**, 184514 (2009).
- ⁴⁸G. M. Luke and Y. J. Uemura (private communications).
- ⁴⁹T. J. Williams *et al.*, *Phys. Rev. B* **82**, 094512 (2010).